Computational Insights into the Formation and Structure of S−N Containing Cyclic Peptides

Sedat Karabulut, Dananjana V. Wijerathne, and James W. Gauld*
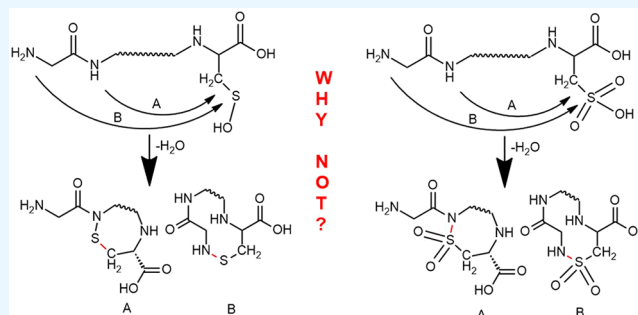
Read Online

ACCESS | Metrics & More | Article Recommendations | Supporting Information

ABSTRACT: Cyclic peptides are known to have biologically important roles and may also be applicable to the pharmaceutical and other industries. Furthermore, thiols and amines, which are found throughout biological systems, can react to form S−N bonds and to date, ~100 biomolecules containing such a bond have been identified. However, while there are in principle numerous S−N containing peptide-derived rings possible, only a few are presently known to occur in biochemical systems. Density functional theory-based calculations have been used to consider the formation and structure of S−N containing cyclic peptides from systematic series of linear peptides in which a cysteinyl has first been oxidized to a sulfenic or sulfonic acid. In addition, the possible effect of the cysteine's vicinal residue on the free energy of formation has also been considered. In general, when the cysteine is first oxidized to a sulfenic acid, only the formation of smaller S−N containing rings is calculated to be exergonic in aqueous solution. In contrast, when the cysteine is first oxidized to a sulfonic acid, the formation of all rings considered (with one exception) is calculated to be endergonic in aqueous solution. The nature of vicinal residue can influence ring formation through stabilizing or destabilizing intramolecular interactions.

INTRODUCTION

Peptides, from small single chains to large protein complexes, are ubiquitous in all organisms. Furthermore, they perform a broad range of essential functions including structural, catalytic, and transportation. In addition, they can also be involved in signaling,[1] act as antimicrobial agents,[2] or more.[3−5] Central to their ability to perform such a myriad of roles is their chemical functionality and structure.

To maintain their structure and thus enable them to function as required, peptides use a range of noncovalent interactions such as electrostatic, $\pi\cdots\pi$, and hydrogen bonds. In addition, their inter- and/or intrapeptide covalent cross-links can also be important for their structure and activity.[6] Indeed, extracellular proteins such as collagen may have a variety of such cross-links and these are critical to their function and even evolution.[7] Of the aforementioned covalent cross-links, disulfide bonds are among the most well-known.[8] However, numerous other types of cross-links can occur in peptides, though to a lesser prevalence, such as isopeptide bonds.[9,10] Recently, experimental studies on a transaldolase enzyme from *Neisseria gonorrhoeae* observed that it exploits reversible redox formation of a −N−O−S− covalent bond bridge between a lysine and cysteine.[6,11]

Despite the prevalence of thiols and amines in nature, S−N bonds are among the most uncommon types of inter- or intramolecular cross-links.[12] In contrast, it has long been known that synthetically, such bonds can be formed under relatively gentle conditions and are widespread in industry and pharmaceuticals.[13−15] At present, while only approximately 100 S−N containing biomolecules are known, there is increasing evidence for their diverse and biologically important roles.[16,17] In fact, such species are now known to play critical roles in the extracellular matrix (e.g., collagen IV),[18] cellular signaling (e.g. S-Nitrosothiols),[19] as neurotoxins (e.g., methionine sulfoximine),[20] anti-inflammatory drugs,[21] or antibiotics.[16] The *Escherichia coli* transcriptional factor protein NemR can reversibly form a S−N containing sulfenylamide (or sulfenamide) cross-link upon exposure to reactive chlorine species.[22] It has been reported that the five-membered S−N containing cycle is performing well under in vitro pharmaco-kinetic studies.[23] Arguably, the most common sulfenylamide found in proteins is also the five-membered ring 1,2-thiazolidin-3-one formed between a cysteinyl and an adjacent amide backbone nitrogen. It was first experimentally observed in the enzyme protein tyrosine phosphatase 1B (PTP1B).[24]
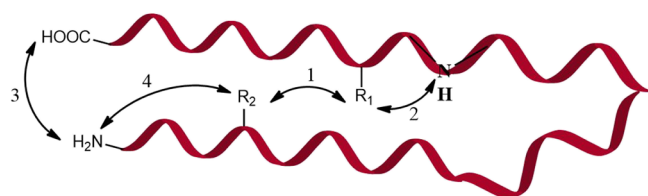
Such examples of peptide-derived sulfenylamide formation raise the tantalizing possibility of cyclic peptides with ring sizes determined by the positions of the thiol sulfur and nitrogen atoms. They also raise the question as to why larger ring sizes are unknown *in vivo*. It is noted that cysteinyls, due to their thiol's rich reactivity,[19,25,26] have long been attractive targets within peptides for modification, including cyclization.[27,28] Meanwhile, cyclic peptides have themselves been shown to be able to possess unique properties such as surface areas with modified polarity, cell permeability, or enhanced binding affinity, bioactivity, and specificity due potentially to greater rigidity.[4,29−32] Indeed, a number of naturally occurring cyclic peptides have been shown to exhibit antibacterial or antitumor activity.[3,5,8,27,33,34] Meanwhile, synthetic cyclic peptides have also long been studied for their potential use as therapeutic agents.[30,35−37] So far, more than 40 cyclic peptides have been approved by the FDA and EMA for clinical treatment.[38]

S−N containing compounds are also able to form diverse chiral structures due to their multiple oxidation states, including many S(IV) and S(VI) stereogenic centers, which are usually neglected by drug discovery programs. These stereogenic centers are underexplored as pharmacophores even though they can significantly increase the structural diversity and complexity of drug candidates.[39] Given the potential chemistry available via S−N bonds,[40] e.g., reversible formation and functionalization, coupled with the biological and pharmaceutical current and potential uses of cyclic peptides,[3,4,41] there is a need to understand the factors that may be important for the formation of cyclic peptides via such bonds.[15] These insights would also be important for aiding experimental identification and isolation of such S−N containing macrocyclic species beyond the limited examples so far experimentally known. Unfortunately, at this time, little information is known including such fundamental aspects as what thermochemical factors may potentially favor the experimentally observed formation of five-membered cyclic sulfenylamides over larger rings or how the residues involved may influence ring formation.

In principle, if only the positions of the to-be-cross-linked groups are considered, peptide cyclization can arise from (1) the side chains of two residues, (2) a side chain and backbone group, (3) the two termini of the peptide, and (4) a residue's side chain and either peptide termini (Scheme 1). In this

Scheme 1. Schematic Illustration of the Possible Cyclizations that May Occur within a Single Peptide

present study, we have used density functional theory-based approaches to examine peptide-derived cyclic sulfenylamide/sulfonamide species. More specifically, we have considered, from a thermodynamic perspective, the effects of the position of the cysteinyl involved (i.e., N- or C-terminus), the oxidation state of the thiol (sulfenic or sulfonic acid), the position and nature of the nitrogen involved (i.e., amide backbone or N-terminus), and effects of the adjacent residue (i.e., glycine,

lysine, serine, tyrosine, arginine, and glutamic acid) on the cyclic sulfenylamide formation.

■ COMPUTATIONAL METHODS

The Molecular Operating Environment (MOE)[42] software package was used to prepare all molecular structures for further study. To help ensure a good initial structure for further study, structures were manually generated and then minimized using the Amber10:EHT molecular mechanics force field, within MOE, due to its ability to reliably model proteins. The Gaussian 16[43] software package was then used to perform all subsequent DFT optimizations, frequencies, and single point energy (SPE) calculations in gas ($\varepsilon = 1.0$), protein ($\varepsilon = 4.0$), and water ($\varepsilon = 78.35$) phases. Optimized structures, of all species considered, were then obtained using the widely used hybrid B3LYP[44] functional in combination with the 6-31 + G(d,p) and 6-311 + G(d,p) basis sets. Optimized geometry at the 6-31 + G(d,p) level was used as the input geometry of 6-311 + G(d,p) optimization. As similar trends were observed in the optimized structures for both basis sets and in all environments, only those obtained geometries using the more extensive 6-311 + G(d,p) basis set and in an aqueous environment ($\varepsilon = 78.35$) are discussed herein unless otherwise noted; however, all optimized structures are provided in the Supporting Information. Harmonic vibrational frequencies were also obtained at these levels of theory to confirm that the structures were minimized and to obtain Gibbs free energy corrections. Relative energies were then obtained by performing single point energy (SP) calculations on the B3LYP/6-311 + G(d,p) optimized structures using the ωB97XD functional in combination with the more extensive 6-311 + G(2df,p) basis set. That is, they were obtained at the ωB97XD/6−311 + G(2df,p)//B3LYP/6-311 + G(d,p) level of theory and corrected to obtain Gibbs free energies in the aqueous phase. It is noted that relative energies were also obtained using the M062X functional for the SP calculations, and similar trends were observed (see the Supporting Information).
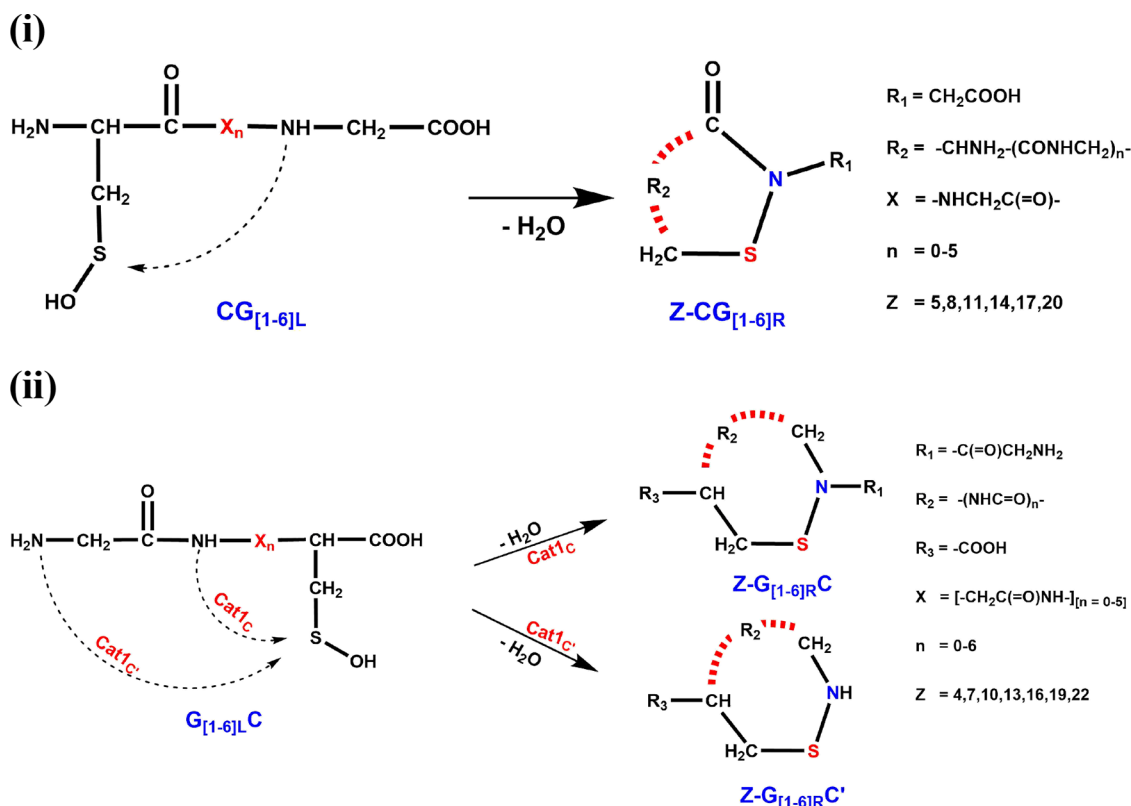
The processes considered herein by which the linear peptide may be converted to a peptide macrocycle, where a water molecule removal accompanies, fall into three categories:

1. Cysteinyl-Derived Sulfenic Acid Acts as an Electrophile (Cat1). This possibility is analogous to the role of sulfenic acid in the PTP1B enzyme[24,45,46] and is illustrated in Scheme 2. This category can be further divided based on the relative position of the cysteinyl sulfenic acid: (i) N- or (ii) C-terminus. For all case studies in group (i), the backbone nitrogen closest to the C-terminus has been considered as the nucleophile (see Scheme 2(i)). Meanwhile, for all case studies in group (ii), the primary N-terminus nitrogen or secondary backbone nitrogen next in the peptide sequence has been considered as the nucleophile (see Scheme 2(ii)).

2. Cysteinyl-Derived Sulfonic Acid Acts as an Electrophile (Cat2). In these, the cysteinyl in the initial linear peptide has been oxidized to a sulfonic acid. As a result, the macrocycle formed contains a sulfonamide, which is an important functional group in, for example, pharmacology.[47] As for the above category, this group can be further sub-divided based on whether the sulfonic acid is at the N- or C-terminus, and possible reactions are illustrated in Scheme 3.

3. Variation of the Vicinal Amino Acid in Cyclizations Involving a Cysteinyl-Derived Sulfenic Acid. In categories 1 and 2 above, glycine was the only other amino acid in the peptide chain. In this group, we considered peptide chains of 2

Scheme 2. Schematic Illustration of the Possible Cyclization Pathways Considered Herein Where the Sulfenic Acid Is at the (i) N- (Cat1$_N$) or (ii) C-Terminus (Cat1$_C$)[a]

(i)

R$_1$ = CH$_2$COOH

R$_2$ = -CHNH$_2$-(CONHCH$_2$)$_n$-

X = -NHCH$_2$C(=O)-

n = 0-5

Z = 5,8,11,14,17,20

(ii)

R$_1$ = -C(=O)CH$_2$NH$_2$

R$_2$ = -(NHC=O)$_n$-

R$_3$ = -COOH

X = [-CH$_2$C(=O)NH-]$_{[n = 0-5]}$

n = 0-6

Z = 4,7,10,13,16,19,22

[a]Z-CG$_{xR(L)}$ (x = 1−6): R/L = ring or linear; ′ indicates that the nucleophile is the N-terminus nitrogen; Z = ring size.

and 3 amino acid residues in length, in which the vicinal or C-terminus residue was replaced by serine, arginine, tyrosine, lysine, or glutamic acid. Lysine, arginine, and glutamic acid were considered in their common charged states, and residues were selected to represent charged, neutral polar, and neutral nonpolar residues. The possible reactions are illustrated in Scheme 4.

Collectively, these models gave S−N containing cyclic peptides of varying ring size from 4 to 22.
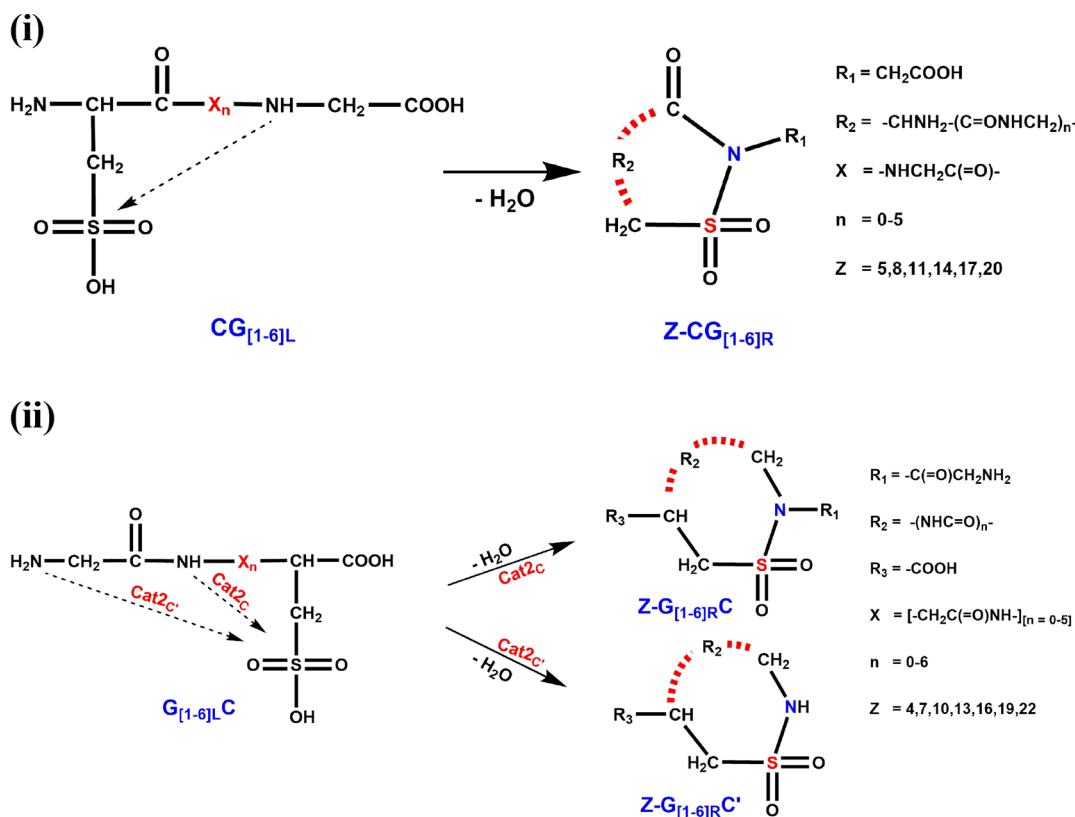
■ RESULTS AND DISCUSSION

Structure and Gibb's Free Energies for Cat1 Cyclization. In these compounds, as noted in the Computational Methods, the putative initial cysteinyl thiol is in its sulfenic acid form and is at the N (Cat1$_N$) or C-terminus (Cat1$_C$) position, and all other residues in the peptide are glycine. The former group, Cat1$_N$, represents all presently known naturally occurring protein-derived sulfenylamides, i.e., 5-membered rings. Thus, this study begins with examining their structures and relative free energies (see Table 1). Characteristic angles, dihedral angles, and bond lengths were reported on this table with ΔG (Gibbs free energy of cyclization reaction).

In the systematic series of Cat1$_N$, the ring formed contains an amide bond adjacent to the S−N bond (see Table 1). The smallest possible ring of this series is 5-membered (5-CG$_R$) and is, as can be seen in Table 1, structurally distinct from all the other systematically larger Cat1$_N$ rings. For example, its S−N bond is the longest of all Cat1$_N$ rings at 1.762 Å, while concomitantly, it possesses the shortest C$_b$−N bond at 1.361 Å
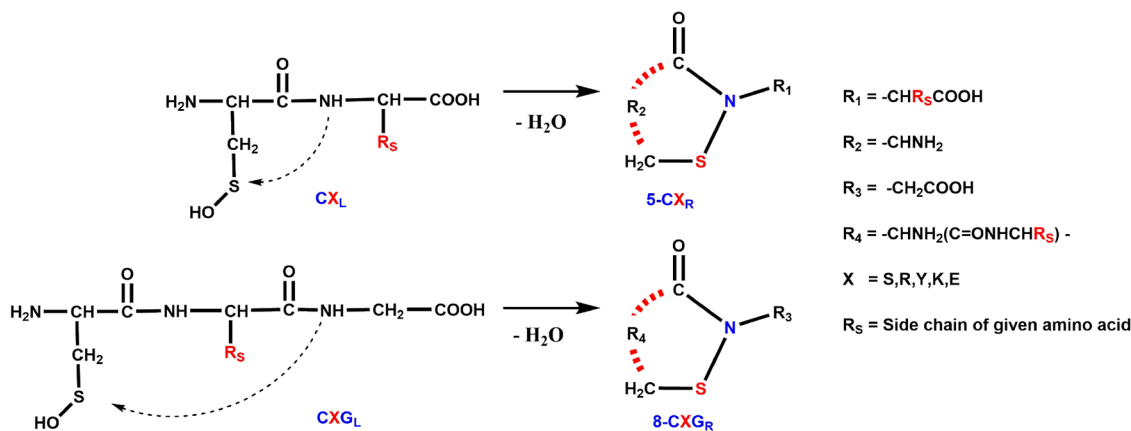
and may explain the stability ($\Delta G = -11.1$ kcal/mol) of cyclic analog with more conjugation of nitrogen lone pairs. In the experimentally reported X-ray structure of the 5-membered sulfenylamide in for PTP1B (PDB ID: 1OES),[24] the S−N and C−N distances are 1.64 and 1.34 Å, respectively. These differ from those detailed above due in part to differences in environmental polarity and the vicinal residue, as well as intramolecular interactions (Scheme S2) in the experimental sulfenylamide PTP1B structure that are not present in the present models. However, it is also noted that our values are in close agreement with those we obtained, 1.758 and 1.356 Å, for the 5-membered sulfenylamide ring in PTP1B using QM/MM.[48] Meanwhile, the ∠C$_b$-N-S and ∠N-S-C$_a$ angles in 5-CG$_R$ are also the smallest of all Cat1$_N$ rings at 115.4 and 89.2°, respectively, highlighting the strained nature of the 5-membered ring. Indeed, expanding the ring by 3 to form 8-CG$_{2R}$, a marked shortening of the S−N bond is observed by 0.025 to 1.737 Å, while the C−N bond lengthens by 0.014 to 1.375 Å. Meanwhile, the largest single increases in ∠C$_b$-N-S and ∠N-S-C$_a$ are also observed, which increase to 126.9 and 102.4°, respectively. If all the rings assumed to be planar, the ∠C$_b$-N-S and ∠N-S-C$_a$ angles would be 108, 135, 147.27, 154, 158, 82, and 162 (180-(360/ring size)). Thus, the 5-CG$_R$ and 8-CG$_{2R}$ are the most similar cyclic peptides to planar versions, and it is observed that there is a significant amount of deviation from planarity for larger rings. The largest changes observed, in these bond lengths and angles, upon further systematic increases in the Cat1$_N$ ring occurs in the C$_b$−N bond, which further increase to 1.391 Å (14-CG$_{4R}$) before shortening slightly to 1.373 Å (17-CG$_{5R}$). The short C$_b$−N length in all

Scheme 3. Schematic Illustration of the Possible Cyclization Pathways Considered Herein Where the Sulfenic Acid Is at the (i) N- (Cat2$_N$) or (ii) C-Terminus (Cat2$_C$)[a]

(i)

$R_1 = CH_2COOH$

$R_2 = -CHNH_2-(C=ONHCH_2)_n-$

$X = -NHCH_2C(=O)-$

$n = 0-5$

$Z = 5,8,11,14,17,20$

CG$_{[1-6]L}$ Z-CG$_{[1-6]R}$

(ii)

$R_1 = -C(=O)CH_2NH_2$

$R_2 = -(NHC=O)_n-$

$R_3 = -COOH$

$X = [-CH_2C(=O)NH-]_{[n = 0-5]}$

$n = 0-6$

$Z = 4,7,10,13,16,19,22$

G$_{[1-6]L}$C   Z-G$_{[1-6]R}$C

Z-G$_{[1-6]R}$C'

[a] Z-CG$_{xR(L)}$ ($x = 1-6$): R/L = ring or linear; ' indicates that the nucleophile is the N-terminus nitrogen; Z = ring size.

Scheme 4. Schematic Illustration of the Possible Cyclization Pathways Considered Herein Where the Sulfenic Acid Is at the N-Terminus, and the Adjacent of C-Terminus Residue Is Serine, Arginine, Tyrosine, Lysine, or Glutamic Acid[a]
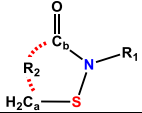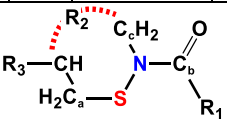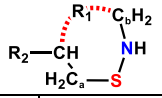

$R_1 = -CHR_SCOOH$

$R_2 = -CHNH_2$

$R_3 = -CH_2COOH$

$R_4 = -CHNH_2(C=ONHCHR_S)-$

$X = S,R,Y,K,E$

R_S = Side chain of given amino acid

CX$_L$ 5-CX$_R$

CXG$_L$ 8-CXG$_R$

[a] CX$_{yL}$ ($y = 1$ or 2) or Z-CXG$_{yR}$; X = S, R, Y, K, E indicates the residues and peptide length involved in the cyclization; R/L = ring or linear; ' indicates that the nucleophile is the N-terminus nitrogen; Z = ring size.

Cat1$_N$ systems illustrates the amount of conjugation occurring across the C_b center, i.e., the C_b–N bond in the amide N—$C_b(=O)$ group has some double-bond character, which also effects the planarity, and vice versa.

Of the **Cat1$_N$** species considered, the 5-CG$_R$ is calculated, in an aqueous environment, to have the lowest relative Gibb's free energy (ΔG) at −11.7 kcal/mol (Table 1), that is, formation of the 5-**CG$_R$** to be exergonic. The only other **Cat1$_N$** macrocycle formation also found to be exergonic is the next smallest (8-membered) system but only just at −0.7 kcal/mol.

The formation of all other larger **Cat1$_N$** macrocycles (11−20) is calculated to be endergonic by at least 1.6 to 10.1 kcal/mol (see Table 1). Another important thing which should be mentioned about the **Cat1$_N$** compounds is the nonlinearity of ring size and ΔG. As it can be observed on Table 1, ΔG is increasing until 14-CG$_{4R}$ but it reduces again. It can be concluded that there is a competition between the stability of linear and ring analogs for an endergonic or exergonic ΔG. The effect of folding of linear analogs are effective on the increasing ΔG along from 5 to 14 membered rings, but in 17- and 20-

Table 1. Selected Optimized Parameters (($\varepsilon = 78.35$)-B3LYP/6−311 + G(d,p)) of the Cat1$_N$, Cat1$_C$, and Cat1$_{C'}$ Systems and Relative (to the Corresponding Initial Linear Chain) Gibb's Free Energies (ΔG; kcal/mol) in the Aqueous Phase (See Computational Methods)

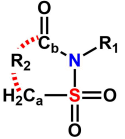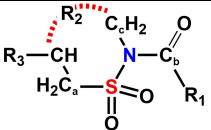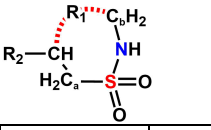| Name							
				R$_1$ = -CH$_2$COOH R$_2$ = -CHNH$_2$(CONHCH$_2$)$_n$ - (n = 0, 1, 2, 3, 4, 5)			
Cat1$_N$	n	**Bond Length (Å)**		**Bond Angle**		**Dihedral**	**ΔG (aq)**
		C$_b$−N	S−N	∠C$_b$-N-S	∠N-S-C$_a$	∠O-C$_b$-N-S	
5-CG$_R$	0	1.361	1.762	115.4	89.2	-179.8	-11.1
8-CG$_{2R}$	1	1.375	1.737	126.9	102.4	-176.1	-0.7
11-CG$_{3R}$	2	1.380	1.740	123.4	103.4	161.8	1.9
14-CG$_{4R}$	3	1.391	1.741	119.5	100.1	-12.1	10.1
17-CG$_{5R}$	4	1.373	1.743	118.7	102.4	3.7	4.8
20-CG$_{-6R}$	5	1.376	1.732	123.6	102.1	179.4	1.6
				R$_1$ = -CH$_2$NH$_2$ R$_2$ = -(NHCOCH$_2$)$_n$ NHCO- (n = 0, 1, 2, 3, 4) R$_3$ = -COOH **Note: Ring size 4 does not have R$_2$ and C$_c$H$_2$**			
Cat1$_C$		C$_b$−N	S−N	∠C$_c$-N-S	∠N-S-C$_a$	∠O-C$_b$-N-S	ΔG (aq)
4-G$_R$C	N/A	1.352	1.778	131.9	75.8	-161.2	3.8
7-G$_{2R}$C	0	1.388	1.732	124.6	100.8	166.9	-5.9
10-G$_{3R}$C	1	1.388	1.764	117.2	106.9	14.0	10.7
13-G$_{4R}$C	2	1.384	1.737	118.9	102.3	3.7	-0.3
16-G$_{5R}$C	3	1.381	1.737	123.8	103.0	-170.4	1.5
19-G$_{6R}$C	4	1.385	1.730	118.9	103.2	-5.5	13.7
				R$_1$ = -(NHCOCH$_2$)$_n$ NHCO- (n = 0, 1, 2, 3, 4, 5) R$_2$ = -COOH			
Cat1$_{C'}$		C$_b$−N	S−N	∠C$_b$-N-S	∠N-S-C$_a$	∠O-C$_b$-N-S	ΔG (aq)
7-G$_R$C'	0	1.452	1.710	118.9	103.9	-53.3	-12.8
10-G$_{2R}$C'	1	1.472	1.725	118.3	104.4	104.1	-4.3
13-G$_{3R}$C'	2	1.475	1.739	115.6	99.6	124.5	-0.3
16-G$_{4R}$C'	3	1.464	1.722	119.6	101.0	102.8	-4.0
19-G$_{5R}$C'	4	1.465	1.731	115.3	101.3	-117.8	2.3
22-G$_{6R}$C'	5	1.463	1.737	116.1	99.7	-127.1	12.4

membered rings, the situation changes and these rings are large enough to fold like a linear peptide that is why the ring formation becomes more favorable.

The **Cat1$_C$** series of S−N containing macrocycles possess several similar structural features to the **Cat1$_N$** series while also having some distinct differences. In particular, the smallest possible S−N containing ring is again strained though now more so being just a 4-membered ring. In addition, the S−N bond is again connected to an amide group (N−C$_b$(=O)), though now the amide carbon is a substituent rather than a ring carbon (see Table 1). The shortest C$_b$−N and longest S−N bond again occur in the most constrained ring, the 4-G$_R$C, with lengths of 1.352 and 1.778 Å, respectively. Expanding the ring to 7 and higher causes a marked lengthening of C$_b$−N to 1.388 Å with a concomitant considerable shortening of the S−N bond to 1.732 Å. This is expected because 4-G$_R$C must be more planar because of the ring size restriction and the exocyclic amide has rotational freedom to orient for best conjugation geometry between nitrogen lone pairs and amide carbon. With only one exception, for the 10-membered ring

system, these bond lengths do not change much as the ring is further expanded. As for the analogous **Cat1$_N$** systems, the short C$_b$−N length again indicates that its increased double bond character is due to delocalization occurring across the C$_b$ center in the N−C$_b$(=O) amide group. Unlike the **Cat1$_N$** series, the smallest **Cat1$_C$** ring (4-G$_R$C) is not the lowest in relative free energy and is in fact slightly unfavored by 3.8 kcal/mol. Instead, the less-constrained 7-G$_{2R}$C has the lowest relative free energy at −5.9 kcal/mol. Each of the larger rings are disfavored by 1.5−13.7 kcal/mol except for 13 membered rings 13-G$_{4R}$C and 13-G$_{3R}$C', which are essentially thermoneutral at −0.3 kcal/mol.

Due in part to their lack of amide group adjacent to the S−N bond, the related **Cat1$_{C'}$** series exhibits some different structural trends. For instance, the shortest C$_b$−N bond is again found in the smallest possible ring (7-G$_R$C'). Now, however, its length is that of a C−N single-bond at 1.452 Å. Furthermore, unlike in the above **Cat1$_N$** and **Cat1$_C$** series, 7-G$_R$C' also contains the shortest S−N bond, which has a length of 1.710 Å. However, as was observed for both the **Cat1$_N$** and

Table 2. Selected Optimized Parameters ((ε = 78.35)-B3LYP/6−311 + G(d,p)) of the Cat2$_N$, Cat2$_C$, and Cat2$_{C'}$ Systems and Relative (to the Corresponding Initial Linear Chain) Gibb's Free Energies (ΔG; kcal/mol) in the Aqueous Phase (See Computational Methods)
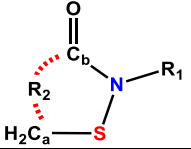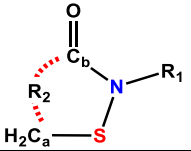
Name				R$_1$ = -CH$_2$COOH R$_2$ = -CHNH$_2$(CONHCH$_2$)$_n$ - (n = 0, 1, 2, 3, 4, 5)		

Cat2$_N$	Bond Length (Å)		Bond Angle		Dihedral	ΔG (aq)
	C$_b$−N	S−N	∠C$_b$-N-S	∠N-S-C$_a$	∠O-C$_b$-N-S	
5-CG$_R$	1.378	1.727	114.5	92.6	176.5	8.1
8-CG$_{2R}$	1.398	1.749	128.4	104.8	-176.4	14.9
11-CG$_{3R}$	1.406	1.740	127.9	106.7	162.7	23.8
14-CG$_{4R}$	1.420	1.735	123.9	104.7	-23.0	27.1
17-CG$_{5R}$	1.412	1.736	127.8	104.6	4.7	20.6
20-CG-$_{6R}$	1.406	1.739	125.4	103.9	172.6	12.9

				R$_1$ = -CH$_2$NH$_2$ R$_2$ = -(NHCOCH$_2$)$_n$ NHCO- (n = 0, 1, 2, 3, 4) R$_3$ = -COOH **Note: Ring size 4 does not have R$_2$ and C$_c$H$_2$**		

Cat2$_C$	C$_b$−N	S−N	∠C$_c$-N-S	∠N-S-C$_a$	∠O-C$_b$-N-S	ΔG (aq)
4-G$_R$C	1.384	1.749	96.1	77.7	-162.9	11.8
7-G$_{2R}$C	1.411	1.738	114.1	101.9	164.7	13.6
10-G$_{3R}$C	1.400	1.763	115.3	109.3	17.6	25.0
13-G$_{4R}$C	1.396	1.742	117.4	105.0	3.8	15.1
16-G$_{5R}$C	1.412	1.737	116.0	105.0	-165.0	24.6
19-G$_{6R}$C	1.392	1.737	117.0	105.7	-4.0	29.6

				R$_1$ = -(NHCOCH$_2$)$_n$ NHCO- (n = 0, 1, 2, 3, 4, 5) R$_2$ = -COOH		

Cat2$_{C'}$	C$_b$−N	S−N	∠C$_b$-N-S	∠N-S-C$_a$	∠O-C$_b$-N-S	ΔG (aq)
7-G$_R$C'	1.460	1.665	119.5	105.7	-53.2	-4.2
10-G$_{2R}$C'	1.475	1.678	121.2	106.1	86.4	4.1
13-G$_{3R}$C'	1.481	1.695	114.2	102.6	175.1	6.4
16-G$_{4R}$C'	1.464	1.674	123.2	102.7	88.1	3.5
19-G$_{5R}$C'	1.470	1.674	119.5	102.4	-136.0	12.6
22-G$_{6R}$C'	1.465	1.673	118.7	102.9	-91.9	17.0

Cat1$_C$ series, 7-G$_R$C′ also has C$_b$−N and S−N lengths that are distinctly differed to all larger Cat1$_{C'}$ macrocycles, despite its apparent reduced ring strain. Systematically, expanding the ring size by 3 to 10, 13, 16, 19, and 22 results in a lengthening of both the C$_b$−N and S−N bonds by at least 0.01 Å (see Table 1). The longest C$_b$−N and S−N bonds occur for the 13-membered ring (13-G$_{3R}$C′) species with lengths of 1.475 and 1.739 Å, respectively. It is noted that with a few exceptions, for all three possible macrocycles types (Cat1$_N$, Cat1$_C$, Cat1$_{C'}$), once the ring is expanded beyond their smallest, the S−N bond length is quite consistently in the range of 1.73−1.74 Å. Energetically, formation of the 7, 10, 13, and 16-membered Cat1$_{C'}$ cyclic peptides are all calculated to be exergonic, with the smallest ring (7-G$_R$C′) being most preferred with −12.8 kcal/mol (Table 1). Of all S−N containing cyclic peptides considered herein, 7-G$_R$C′ is the lowest energy, though it is only slightly lower in energy (1.7 kcal/mol) than the 5-CG$_R$. The latter is, to date, the only one experimentally observed in

protein X-ray crystal structures.[24,45] Formation of the largest Cat1$_{C'}$ macrocycles (19 and 22) are both calculated to be endergonic by 2.3 and 12.4 kcal/mol, respectively.

It is noted that in general, for Cat1 macrocycles, formation of the smallest rings is exergonic, while larger rings are endergonic. Indeed, for both Cat1$_N$ and Cat1$_{C'}$ macrocycles, the smallest possible ring is the most preferred, 5- and 7-membered, respectively. For Cat1$_C$, the second smallest possible ring (7-membered) is preferred. These results in part reflect the ability of various macrocycles to form intramolecular hydrogen bonds; such bonds are not possible in a 4-membered ring but are in a 7-membered ring, etc. In addition, sulfur's nature and variable hybridization may help contribute to the stabilization of the rings (e.g., strain in smaller rings). We also examined energetic changes of formation of these same rings in the gas phase (ε = 1.0) and protein (ε = 4.0) environments, i.e., less polar environments (Table S3). In all cases, the peptide cyclizations were all more

Table 3. Selected Optimized Parameters ((ε = 78.35)-B3LYP/6−311 + G(d,p)) of the Cat3 Systems and Relative (to the Corresponding Initial Linear Chain) Gibb's Free Energies (ΔG; kcal/mol) in the Aqueous Phase (See Computational Methods)

	Bond Length (Å)		ΔG
Cat3$_N$	**C_b−N**	**S−N**	**Water**
5-CK$_R$	1.350	1.771	-13.0
5-CY$_R$	1.359	1.764	-10.5
5-CS$_R$	1.362	1.774	-7.1
5-CR$_R$	1.366	1.766	-5.2
5-CE$_R$	1.355	1.763	-3.5

R$_1$ = -CHR$_s$COOH
R$_2$ = -CHNH$_2$
R$_s$= Side chain of given amino acid

R$_1$ = -CH$_2$COOH
R$_2$ = -CHNH$_2$(CONHCHR$_s$) −
R$_s$= Side chain of given amino acid

8-CKG$_R$	1.380	1.751	4.6
8-CYG$_R$	1.380	1.753	6.0
8-CSG$_R$	1.378	1.731	1.4
8-CRG$_R$	1.370	1.753	1.0
8-CEG$_R$	1.378	1.751	6.4

favored in the more polar aqueous environment. Setting aside possible challenges with ring formation internal to a protein, these results suggest that such ring formation is preferred in more polar environments (e.g., aqueous solvent exposed areas).

It is noted that structurally, the length of the S−N bonds in all **Cat1** systems tend toward that obtained for the unstrained "isolated" system, which is also without an S−N-adjacent amide bond, CH$_3$S−NH$_2$ (r(S−N) = 1.739 Å calculated with the same methodology). Meanwhile the C$_b$−N bond lengths in **Cat1$_N$** and **Cat1$_C$**, while clearly having a significant double bond character, tend toward being approximately 0.03 Å longer than in CH$_3$C(=O)—NH$_2$ (1.353 Å), i.e., have, but less, a double-bond character (Table 1).

Structure and Gibb's Free Energies for Cat2 Cyclic Peptides. As noted above, these macrocycles are formed by cyclization of a parent peptide in which its cysteinyl has been oxidized to a sulfonic acid. The resulting ring thus contains a sulfonamide group, −S(O$_2$)−N− and can alternately be viewed as the oxidized products of **Cat1** macrocycles. Sulfonamides have been experimentally well characterized and are synthetically accessible and pharmaceutically important.[49] Hence, this cyclization could present a new pathway to their formation. The results obtained for S−N containing macrocycles formed this way are shown in Table 2.

As can be seen in Table 2, several of the same trends are observed for the **Cat2** macrocycle series as describe above for their analogous **Cat1** series, although with some key differences. First, the C$_b$−N lengths in the amide group adjacent to the S−N bond in **Cat2$_N$** and **Cat2$_C$** again indicate that it has a double bond character that is reduced slightly as the ring is expanded from the smallest (5-CG$_R$ and 4-CG$_R$).

However, the double bond character in all **Cat2$_N$** and **Cat2$_C$** species is now much reduced. This is illustrated by the fact that upon expanding, for the rings in both systems from 5- to 8-CG$_{1-2R}$ (**Cat2$_N$**) and 4- to 7-G$_R$C (**Cat2$_C$**) (i.e., from smallest to next largest) the length of their C$_b$−N bonds increase by 0.020−0.027 to ~1.40−1.41 Å. For comparison, in 8-CG$_{2R}$ (**Cat1$_N$**) and 7-G$_{2R}$C (**Cat1$_C$**), the C$_b$−N lengths are just 1.375 and 1.388 Å, respectively (cf. Table 1). Meanwhile, the optimized C$_b$−N length of CH$_3$C$_b$(O)−NH$_2$ is 1.353 Å. In contrast, in the **Cat2$_{C'}$** rings, which do not contain a S−N-adjacent amide group, their C$_b$−N lengths are all much longer, ranging from 1.460 to 1.481 Å, that is, they have lengths indicative of a C−N single bond (Table 2).

With regards to the S−N bonds in the **Cat2$_N$** cyclic peptides, i.e., contain an amide bond adjacent to the S−N moiety, the shortest S−N bond (1.727 Å) is found in the smallest ring, 5-CG$_R$ (**Cat2$_N$**). Expanding the ring causes a lengthening in the bond to lie in the range of 1.735−1.749 Å, depending on the ring size. The S−N bond length appears to converge toward 1.74 Å as the ring is systematically expanded. However, regardless of the ring size, all of these S−N bonds are longer than obtained for the optimized structure of the linear aqueous analog CH$_3$S(O)$_2$—NC$_b$(=O)CH$_3$; r(S−N) = 1.702 Å. This suggests that the S−N bond in the **Cat2$_N$** rings considered is slightly weakened.

The **Cat2$_C$** macrocycles also have an amide group adjacent to the S−N bond. However, in the smallest **Cat2$_C$** ring, the 4-membered 4-G$_R$C (**Cat2$_C$**), the S−N bond is quite a bit longer at 1.749 Å (Table 2). Systematically expanding the ring, at least initially to a 7- and then 10-membered ring, causes first a slight decrease in the S−N bond length from 1.749 to 1.738 Å then an increase to 1.763 Å. It then shortens to lie in the range of

1.742−1.737 Å upon further expanding to 13-, 16-, and 19-membered rings. Again, as in the $\mathbf{Cat2_N}$ series, these values all suggest that the S−N bond is slightly weakened in the $\mathbf{Cat2_C}$ macrocycles likely due to the presence of the S−N adjacent substituted amide group. Indeed, in the smallest $\mathbf{Cat2_{C'}}$ ring (7-$\mathbf{G_RC'}$), which has no amide group adjacent to the S−N bond, its S−N bond is markedly shorter at 1.665 Å. Systematically expanding the ring to 10- and 13- causes the S−N bond to lengthen to 1.678 and 1.695 Å, respectively (Table 2). Further expanding the ring to 13-, 16-, and 19-, however, causes it to shorten to 1.673−1.674 Å. These lengths are in close agreement with the optimized (see Computational Methods) length of the S−N bond in the linear model $CH_3SO_2−NH_2$; 1.680 Å.

For all three ($\mathbf{Cat2_N}$, $\mathbf{Cat2_C}$, and $\mathbf{Cat2_{C'}}$) cyclic peptide systems of $\mathbf{Cat2}$, their smallest possible ring system is also energetically the most preferred with relative Gibbs free energies (ΔG) of 8.1, 11.8, and −4.2 kcal/mol, respectively (Table 2). Thus, as for the analogous $\mathbf{Cat1}$ systems, for all $\mathbf{Cat2}$ systems, the 7-membered $\mathbf{Cat2_{C'}}$ ring (7-$\mathbf{G_RC'}$) is calculated to have the lowest ΔG. However, unlike that observed for the $\mathbf{Cat1}$ macrocycles, 7-$\mathbf{G_RC'}$ is the only $\mathbf{Cat2}$ system whose ring formation from the corresponding linear parent is calculated to be exergonic. That is, it is the only system for which ring formation is calculated to be favored. Indeed, all $\mathbf{Cat2}$ macrocycles, including 7-$\mathbf{G_RC'}$, are calculated to lie higher in relative free energy than their corresponding $\mathbf{Cat1}$ macrocycle. That is, sulfonamide containing cyclic peptide formation is less favorable than sulfenylamide. It is noted that in general, however, within the $\mathbf{Cat2}$ systems, those without an amide group adjacent to the S−N bond (i.e., $\mathbf{Cat2_{C'}}$) have lower calculated ΔG values than the other $\mathbf{Cat2}$ systems considered herein (see Table 2).

Effects of Varying the Vicinal Amino Acid in Cyclizations via a Cysteinyl-Derived Sulfenic Acid. Each of the above peptides considered ($\mathbf{Cat1}$ and $\mathbf{Cat2}$) consists of a single cysteine while all others are glycine residues. Thus, to consider the effects of changing the vicinal residue, we examine di- and tripeptides in which residue adjacent to the cysteine was varied (i.e., Lys, tyrosine, serine, arginine, and glutamic acid) and subsequently, 5- and 8-membered macrocycles were formed and hereafter referred to as $\mathbf{Cat3}$ macrocycles (see Table 3). These substitutions introduce different side-chain functionalities as well as greater conformational constraint that may impact the ability to form S−N-derived macrocycles. The results obtained are provided in Table 3. For comparison, one can consider the corresponding 5-membered (5-$\mathbf{CG_R}$; $\mathbf{Cat1_N}$) and 8-membered macrocycle (8-$\mathbf{CG_{2R}}$; $\mathbf{Cat1_N}$) formed from CG and CGG, respectively, as their unsubstituted analogs (cf. Table 1).

In the case of 5-membered ring-containing $\mathbf{Cat3_N}$ cyclic peptides derived from CX dipeptides (X = K, Y, S, R, E), only relatively modest differences were observed in their key $C_b−N$ and S−N bonds, compared to the CG derived 5-$\mathbf{CG_R}$($\mathbf{Cat1_N}$) (cf. Table 1). For example, $C_b−N$ bonds in all 5-$\mathbf{CX_R}$($\mathbf{Cat3_N}$) species again show a marked double-bond character with lengths in the range of 1.350−1.366 Å. In comparison, in 5-$\mathbf{CG_R}$($\mathbf{Cat1_N}$), the analogous bond had an optimized length of 1.361 Å. Meanwhile, the optimized values of the S−N bonds of the 5-$\mathbf{CX_R}$($\mathbf{Cat3_N}$) species lie in the range of 1.763−1.774 Å, while in the 5-$\mathbf{CG_R}$($\mathbf{Cat1_N}$) ring, its length was 1.766 Å (cf. Table 1). That is, for the 5-membered rings formed from the

substituted dipeptides 5-$\mathbf{CX_R}$($\mathbf{Cat3_N}$), the S−N bond is lengthened by only 0.001−0.012 Å.

There is clearly an energetic impact resulting from the choice of vicinal residue. Indeed, the preference for formation of a 5-membered cyclic sulfenylamide is in the order of is CK > CG (Table 1) > CY > CS > CR > CE. That is, in all substituted dipeptides considered, the formation of a 5-membered cyclic sulfenylamide is exergonic, though not equally favored. This ordering does not match the experimentally determined scale of flexibility for amino acids proposed by Huang and Nau,[50] suggesting that other interactions (e.g., hydrogen bonding) may influence their stability. Indeed, in the ring formed within the dipeptide 5-$\mathbf{CK_R}$, the positively charged side chain off the Lys is long and flexible enough for its protonated sidechain to interact with the cysteine carbonyl and is a main stabilizing influence for 5-membered cysteine−lysine dipeptide cyclization (Scheme S1). Meanwhile, when the vicinal residue is glutamic acid, in the ring formed, its anionic sidechain is close to the backbone oxygen and nitrogen due to the structural rigidity of cyclic peptide, thus rendering it the least favored of the exergonic 5-membered ring formations (Table 3). It is noted that in protein tyrosine phosphatase 1B (PTP1B), the 5-membered cyclic sulfenylamide is formed between a cysteine and adjacent serine whose formation is calculated above to be exergonic. According to reported results here, a vicinal serine is not essential for S−N containing cyclization.

For the corresponding 8-membered substituted rings (8-$\mathbf{CXG_R}$) formed from the tripeptides, the $C_b−N$ bonds are all effectively the same (+0.003 − +0.005 Å) as that obtained for the 8-$\mathbf{CG_{2R}}$ (Table 1). Meanwhile, the length of S−N bonds in the 8-$\mathbf{CXG_R}$ systems are all longer than in 8-$\mathbf{CG_{2R}}$ ($\mathbf{Cat1_N}$) by 0.014−0.022 Å. The only exception occurs when the middle residue is serine, which has a slightly shorter S−N bond of 1.731 Å. This is perhaps not unexpected given that in the sequence determined by Huang and Nau,[50] the most flexible residue after glycine is serine. Also, this may be the contributing factor to the PTP1B example. Energetically, however, while the formation of the S−N containing 8-$\mathbf{CG_{2R}}$ macrocycle from $\mathbf{Cat1_N}$ was calculated to be slightly exergonic (−0.7 kcal/mol; Table 1), the formation of all 8-$\mathbf{CXG_R}$ systems considered herein are calculated to be endergonic by 1.4−6.7 kcal/mol. The least disfavored is that formed from 8-$\mathbf{CRG_R}$; serine is the second most favorable with 0.4 kcal/mol difference again for the next most flexible residue and which can also form hydrogen bonds. Meanwhile, the most disfavored are those formed from 8-$\mathbf{CEG_R}$ and 8-$\mathbf{CYG_R}$. That is, where intramolecular hydrogen bonding is either not possible or there are destabilizing intramolecular interactions (i.e., CEG).

■ CONCLUSIONS

Density functional theory-based calculations have been used to study the formation and structure of systematic series of peptide-derived S−N containing rings. Specifically, sulfenylamide (S−N) containing ring formation (ring size = 4−22) in a series of peptides (CG$_n$ or G$_n$C, n = 1−6), with the initial N- or C-terminal cysteine oxidized to a sulfenic acid and then reacted with the C-terminal backbone amide nitrogen ($\mathbf{Cat1_N}$) or N-terminal adjacent backbone amide (−NH−) or N-terminal amine nitrogen ($\mathbf{Cat1_C}$ and $\mathbf{Cat1_{C'}}$ respectively), was considered. Formation of an analogous series of sulfonylamide containing rings was also examined. For these, the initial

cysteine was oxidized to sulfonic acid ($\mathbf{Cat2_N}$, $\mathbf{Cat2_C}$, $\mathbf{Cat2_{C'}}$). Finally, the influence of the vicinal residue to the cysteine was also considered using the di- and tripeptides CX and CXG (X = K, Y, S, R, E).

In general, for S-N containing rings formed via a sulfenic acid ($\mathbf{Cat1}$), only formation of smaller rings gave exergonic ΔG_{aq} values, with the smallest ring possible for each series being the most preferred. These trends reflect several effects including ring strain and ability to form stabilizing intramolecular interactions. The most exergonic $\mathbf{Cat1}$ rings were calculated to be the 5-membered 5-CG$_R$ ($\mathbf{Cat1_N}$) and 7-membered 7-G$_{2R}$C ($\mathbf{Cat1_C}$)/7-G$_{2R}$C$'$ ($\mathbf{Cat1_{C'}}$) rings with ΔG_{aq} values of −11.1, −5.9, and −12.8 kcal/mol, respectively. The formation of larger rings, in general, was endergonic. Notably, the above 5-membered sulfenylamide ring (5-CG$_R$) is analogous to those experimentally observed in some proteins (e.g., PTP1B). Structurally, in the $\mathbf{Cat1_N}$ and $\mathbf{Cat1_C}$ macrocycles, the S−N nitrogen is adjacent to a carbonyl since in the parent linear peptide, it was within an amide. In both series of macrocycles, the longest S−N bond occurs in the smallest ring 5-CGR and 4-GRC with lengths of 1.762 and 1.778 Å, respectively. As the ring is expanded, they shorten dramatically to 1.73 Å. In contrast, in the $\mathbf{Cat1C'}$ series of rings, the S−N nitrogen originated from the N-terminal amine. As a result, in this series, the shortest S−N bond (1.710 Å) occurs in the smallest ring (7-GRC$'$) and lengthens to 1.73−1.74 Å as the ring is expanded.

In contrast, for S−N containing macrocycles formed via a cysteinyl sulfonic acid ($\mathbf{Cat2}$), the formation of all macrocycles was calculated to be endergonic in aqueous solution. The only exception was formation of the 7-membered 7-G$_R$C$'$ ($\mathbf{Cat2_{C'}}$) ring with a ΔG_{aq} of −4.2 kcal/mol.

The nature of the residue vicinal to the cysteine ($\mathbf{Cat3}$) influences the ΔG_{aq} of formation for the 5- and 8-membered rings. More specifically, for the 5-membered cyclic sulfenylamide, the preference of formation (in kcal/mol) is CK (−13.0) > CG (−11.1) > CY (−10.5) > CS (−7.1) > CR (−5.2) > CE (−3.5). In contrast, the only 8-membered ring whose formation was calculated to be exergonic was 8-CG$_{2R}$ (−0.7 kcal/mol), i.e., when the vicinal residue was glycine. The formation of all others considered here was calculated to be endergonic by 1.0−6.4 kcal/mol. While other factors may influence these orderings within a protein environment, these ΔG_{aq} values reflect in part the effect of stabilizing or destabilizing intramolecular interactions in the resulting ring.

Synthetic (cyclo)peptides have been attracting increasing attention, especially in medicinal chemistry. Reported exergonic Gibbs free energies for some of the peptide cyclization may guide synthetic organic chemists. These results are an important step in understanding peptide-derived S−N containing ring systems. In addition, they also provide insights into experimental observations of sulfenylamide rings within peptides, as well as into other possible S−N bond containing macrocycles that may be biologically and/or experimentally accessible and with a variety of potential applications.

■ ASSOCIATED CONTENT

⑤ Supporting Information

The Supporting Information is available free of charge at https://pubs.acs.org/doi/10.1021/acsomega.3c01764.

Calculated ΔG (kcal/mol) results obtained for formation of the cyclic peptides from their corresponding linear peptide, schematic illustration of the intramolecular hydrogen bonding in CK$_R$, and Gaussian archive entries from the (ε = 1.0, 4.0, or 78.35)-ωB97XD/6−311 + g(2df,p)/(ε = 78.35)-B3LYP/6−311 + G(d,p) calculations for all cyclic species (PDF)

■ AUTHOR INFORMATION

Corresponding Author

James W. Gauld − *Department of Chemistry and Biochemistry, University of Windsor, Windsor, Ontario N9B 3P4, Canada;* ⊙ orcid.org/0000-0002-2956-9781; Email: gauld@uwindsor.ca

Authors

Sedat Karabulut − *Department of Chemistry and Biochemistry, University of Windsor, Windsor, Ontario N9B 3P4, Canada*

Dananjana V. Wijerathne − *Department of Chemistry and Biochemistry, University of Windsor, Windsor, Ontario N9B 3P4, Canada*

Complete contact information is available at:
https://pubs.acs.org/10.1021/acsomega.3c01764

Author Contributions

S.K. and D.V.W. did the DFT calculations, analyses, and writing; J.W.G. did the mentoring, analyses, and writing.

Notes

The authors declare no competing financial interest.

■ REFERENCES

(1) Duffaud, G. D.; Lehnhardt, S. K.; March, P. E.; Inouye, M. Chapter 2 Structure and Function of the Signal Peptide. In *Current Topics in Membranes and Transport*, Bronner, F. Ed.; Vol. *24*; Academic Press, New York, 1985; pp. 65−104.

(2) Lau, Y. E.; Rozek, A.; Scott, M. G.; Goosney, D. L.; Davidson, D. J.; Hancock, R. E. W. Interaction and cellular localization of the human host defense peptide LL-37 with lung epithelial cells. *Infect. Immun.* 2005, *73*, 583−591.

(3) Smolyar, I. V.; Yudin, A. K.; Nenajdenko, V. G. Heteroaryl Rings in Peptide Macrocycles. *Chem. Rev.* 2019, *119*, 10032−10240.

(4) Vinogradov, A. A.; Yin, Y.; Suga, H. Macrocyclic Peptides as Drug Candidates: Recent Progress and Remaining Challenges. *J. Am. Chem. Soc.* 2019, *141*, 4167−4181.

(5) Hayes, H. C.; Luk, L. Y. P.; Tsai, Y. H. Approaches for peptide and protein cyclisation. *Org. Biomol. Chem.* 2021, *19*, 3983−4001.

(6) Wensien, M.; Rabe von Pappenheim, F.; Funk, L.-M.; Kloskowski, P.; Curth, U.; Diederichsen, U.; Uranga, J.; Ye, J.; Fang, P.; Pan, K.-T.; Urlaub, H.; Mata, R. A.; Sautner, V.; Tittmann, K. A lysine−cysteine redox switch with an NOS bridge regulates enzyme function. *Nature* 2021, *593*, 460−464.

(7) Rodriguez-Pascual, F.; Slatter, D. A. Collagen cross-linking: Insights on the evolution of metazoan extracellular matrix. *Sci. Rep.* 2016, *6*, 37374.

(8) Wiedemann, C.; Kumar, A.; Lang, A.; Ohlenschläger, O. Cysteines and Disulfide Bonds as Structure-Forming Units: Insights From Different Domains of Life and the Potential for Characterization by NMR. *Front. Chem.* 2020, *8*, 280.

(9) Androutsou, M. E.; Nteli, A.; Gkika, A.; Avloniti, M.; Dagkonaki, A.; Probert, L.; Tselios, T.; Golič Grdadolnik, S. Characterization of Asparagine Deamidation in Immunodominant Myelin Oligodendro-

cyte Glycoprotein Peptide Potential Immunotherapy for the Treatment of Multiple Sclerosis. *Int. J. Mol. Sci.* **2020**, *21*, 7566.

(10) Güttler, B. H.-O.; Cynis, H.; Seifert, F.; Ludwig, H. H.; Porzel, A.; Schilling, S. A quantitative analysis of spontaneous isoaspartate formation from N-terminal asparaginyl and aspartyl residues. *Amino Acids* **2013**, *44*, 1205−1214.

(11) Rabe von Pappenheim, F.; Wensien, M.; Ye, J.; Uranga, J.; Irisarri, I.; de Vries, J.; Funk, L.-M.; Mata, R. A.; Tittmann, K. Widespread occurrence of covalent lysine−cysteine redox switches in proteins. *Nat. Chem. Biol.* **2022**, *18*, 368−375.

(12) Davis, M.; Morris, J. L. Why are S-N bonds so rare in nature? *J. Chem. Educ.* **1981**, *58*, 760.

(13) Villalba, M. L.; Enrique, A. V.; Higgs, J.; Castaño, R. A.; Goicoechea, S.; Taborda, F. D.; Gavernet, L.; Lick, I. D.; Marder, M.; Bruno Blanch, L. E. Novel sulfamides and sulfamates derived from amino esters: Synthetic studies and anticonvulsant activity. *Eur. J. Pharmacol.* **2016**, *774*, 55−63.

(14) *Comprehensive Heterocyclic Chemistry*; Katritzky, A. R., Rees, C. W. Eds.; Vol *1-8*, Pergamon Press: Oxford, 1984.

(15) Wang, B.; Liang, X.; Zeng, Q. Recent Advances in the Synthesis of Cyclic Sulfoximines via C−H Bond Activation. *Molecules* **2023**, *28*, 1367−1390.

(16) Petkowski, J. J.; Bains, W.; Seager, S. Natural Products Containing a Nitrogen-Sulfur Bond. *J. Nat. Prod.* **2018**, *81*, 423−446.

(17) Craine, L.; Raban, M. The Chemistry of Sulfenamides. *Chem. Rev.* **1989**, *89*, 689−712.

(18) Vanacore, R.; Ham, A. J. L.; Voehler, M.; Sanders, C. R.; Conrads, T. P.; Veenstra, T. D.; Sharpless, K. B.; Dawson, P. E.; Hudson, B. G. A Sulfilimine Bond Identified in Collagen IV. *Science* **2009**, *325*, 1230−1234.

(19) Klomsiri, C.; Karplus, P. A.; Poole, L. B. Cysteine-based redox switches in enzymes. *Antioxid. Redox Signaling* **2011**, *14*, 1065−1077.

(20) Ghoddoussi, F.; Galloway, M. P.; Jambekar, A.; Bame, M.; Needleman, R.; Brusilow, W. S. A. Methionine sulfoximine, an inhibitor of glutamine synthetase, lowers brain glutamine and glutamate in a mouse model of ALS. *J. Neurol. Sci.* **2010**, *290*, 41−47.

(21) Xu, S.; Rouzer, C. A.; Marnett, L. J. Oxicams, a class of nonsteroidal anti-inflammatory drugs and beyond. *IUBMB Life* **2014**, *66*, 803−811.

(22) Gray, M. J.; Li, Y.; Leichert, L. I. O.; Xu, Z.; Jakob, U. Does the Transcription Factor NemR Use a Regulatory Sulfenamide Bond to Sense Bleach? *Antioxid. Redox Signaling* **2015**, *23*, 747−754.

(23) Boulard, E.; Zibulski, V.; Oertel, L.; Lienau, P.; Schäfer, M.; Ganzer, U.; Lücking, U. Increasing Complexity: A Practical Synthetic Approach to Three-Dimensional, Cyclic Sulfoximines and First Insights into Their in Vitro Properties. *Chem. − Eur. J.* **2020**, *26*, 4378−4388.

(24) Van Montfort, R. L. M.; Congreve, M.; Tisi, D.; Carr, R.; Jhoti, H. Oxidation state of the active-site cysteine in protein tyrosine phosphatase 1B. *Nature* **2003**, *423*, 773−777.

(25) Bak, D. W.; Bechtel, T. J.; Falco, J. A.; Weerapana, E. Cysteine reactivity across the subcellular universe. *Curr. Opin. Chem. Biol.* **2019**, *48*, 96−105.

(26) Maurais, A. J.; Weerapana, E. Reactive-cysteine profiling for drug discovery. *Curr. Opin. Chem. Biol.* **2019**, *50*, 29−36.

(27) Henninot, A.; Collins, J. C.; Nuss, J. M. The Current State of Peptide Drug Discovery: Back to the Future? *J. Med. Chem.* **2018**, *61*, 1382−1414.

(28) Bošnjak, I.; Bojović, V.; Šegvić-Bubić, T.; Bielen, A. Occurrence of protein disulfide bonds in different domains of life: A comparison of proteins from the Protein Data Bank. *Protein Eng., Des. Sel.* **2014**, *27*, 65−72.

(29) Rezai, T.; Bock, J. E.; Zhou, M. V.; Kalyanaraman, C.; Lokey, R. S.; Jacobson, M. P. Conformational flexibility, internal hydrogen bonding, and passive membrane permeability: Successful in silico prediction of the relative permeabilities of cyclic peptides. *J. Am. Chem. Soc.* **2006**, *128*, 14073−14080.

(30) Joo, S. H. Cyclic peptides as therapeutic agents and biochemical tools. *Biomol. Ther.* **2012**, *20*, 19−26.

(31) Rubin, S. J. S.; Qvit, N. Backbone-Cyclized Peptides: A Critical Review. *Curr. Top. Med. Chem.* **2018**, *18*, 526−555.

(32) Wang, C. K.; Craik, D. J. Designing macrocyclic disulfide-rich peptides for biotechnological applications perspective. *Nat. Chem. Biol.* **2018**, *14*, 417−427.

(33) Ikonomopoulou, M. P.; Fernandez-Rojo, M. A.; Pineda, S. S.; Cabezas-Sainz, P.; Winnen, B.; Morales, R. A. V.; Brust, A.; Sánchez, L.; Alewood, P. F.; Ramm, G. A.; Miles, J. J.; King, G. F. Gomesin inhibits melanoma growth by manipulating key signaling cascades that control cell death and proliferation. *Sci. Rep.* **2018**, *8*, 11519.

(34) Waldman, A. J.; Ng, T. L.; Wang, P.; Balskus, E. P. Heteroatom-Heteroatom Bond Formation in Natural Product Biosynthesis. *Chem. Rev.* **2017**, *117*, 5784−5863.

(35) Sarkar, S.; Gu, W.; Schmidt, E. W. Expanding the Chemical Space of Synthetic Cyclic Peptides Using a Promiscuous Macrocyclase from Prenylagaramide Biosynthesis. *ACS Catal.* **2020**, *10*, 7146−7153.

(36) Ullrich, S.; Sasi, V. M.; Mahawaththa, M. C.; Ekanayake, K. B.; Morewood, R.; George, J.; Shuttleworth, L.; Zhang, X.; Whitefield, C.; Otting, G.; Jackson, C.; Nitsche, C. Challenges of short substrate analogues as SARS-CoV-2 main protease inhibitors. *Bioorg. Med. Chem. Lett.* **2021**, *50*, No. 128333.

(37) Benfield, A. H.; Defaus, S.; Lawrence, N.; Chaousis, S.; Condon, N.; Cheneval, O.; Huang, Y. H.; Chan, L. Y.; Andreu, D.; Craik, D. J.; Henriques, S. T. Cyclic gomesin, a stable redesigned spider peptide able to enter cancer cells. *Biochim. Biophys. Acta, Biomembr.* **2021**, *1863*, No. 183480.

(38) Tao, H.; Wu, Q.; Zhao, X.; Lin, P.; Huang, S.-Y. Efficient 3D conformer generation of cyclic peptides formed by a disulfide bond. *Aust. J. Chem.* **2022**, *14*, 26.

(39) Zhang, X.; Wang, F.; Tan, C.-H. Asymmetric Synthesis of S(IV) and S(VI) Stereogenic Centers. *J. Am. Chem. Soc. Au* **2023**, 700.

(40) Leusser, D.; Henn, J.; Kocher, N.; Engels, B.; Stalke, D. S=N versus S+-N-: An Experimental and Theoretical Charge Density Study. *J. Am. Chem. Soc.* **2004**, *126*, 1781−1793.

(41) Wu, J.; Tang, J.; Chen, H.; He, Y.; Wang, H.; Yao, H. Recent developments in peptide macrocyclization. *Tetrahedron Lett.* **2018**, *59*, 325−333.

(42) *Molecular Operating Environment (MOE)*, 2022.02 Chemical Computing Group ULC, 1010 Sherbrooke St. West, Suite #910, Montreal, QC, Canada, H3A 2R7, 2023.

(43) Frisch, M. J.; Trucks, G. W.; Schlegel, H. B.; Scuseria, G. E.; Robb, M. A.; Cheeseman, J. R.; Scalmani, G.; Barone, V.; Petersson, G. A.; Nakatsuji, H.; Li, X.; Caricato, M.; Marenich, A. V.; Bloino, J.; Janesko, B. G.; Gomperts, R.; Mennucci, B.; Hratchian, H. P.; Ortiz, J. V.; Izmaylov, A. F.; Sonnenberg, J. L.; Williams; Ding, F.; Lipparini, F.; Egidi, F.; Goings, J.; Peng, B.; Petrone, A.; Henderson, T.; Ranasinghe, D.; Zakrzewski, V. G.; Gao, J.; Rega, N.; Zheng, G.; Liang, W.; Hada, M.; Ehara, M.; Toyota, K.; Fukuda, R.; Hasegawa, J.; Ishida, M.; Nakajima, T.; Honda, Y.; Kitao, O.; Nakai, H.; Vreven, T.; Throssell, K.; Montgomery, Jr., J. A.; Peralta, J. E.; Ogliaro, F.; Bearpark, M. J.; Heyd, J. J.; Brothers, E. N.; Kudin, K. N.; Staroverov, V. N.; Keith, T. A.; Kobayashi, R.; Normand, J.; Raghavachari, K.; Rendell, A. P.; Burant, J. C.; Iyengar, S. S.; Tomasi, J.; Cossi, M.; Millam, J. M.; Klene, M.; Adamo, C.; Cammi, R.; Ochterski, J. W.; Martin, R. L.; Morokuma, K.; Farkas, O.; Foresman, J. B.; Fox, D. J. *Gaussian 16 Rev. C.01, Wallingford, CT*, 2016.

(44) Raghavachari, K. Perspective on "Density functional thermochemistry. III. The role of exact exchange". *Theor. Chem. Acc.* **2000**, *103*, 361−363.

(45) Salmeen, A.; Andersen, J. N.; Myers, M. P.; Meng, T. C.; Hinks, J. A.; Tonks, N. K.; Barford, D. Redox regulation of protein tyrosine phosphatase 1B involves a sulphenyl-amide intermediate. *Nature* **2003**, *423*, 769−773.

(46) Salmeen, A.; Barford, D. Functions and Mechanisms of Redox Regulation of Cysteine-Based Phosphatases. *Antioxid. Redox Signaling* **2005**, *7*, 560−577.

(47) Baunach, M.; Ding, L.; Willing, K.; Hertweck, C. Bacterial Synthesis of Unusual Sulfonamide and Sulfone Antibiotics by Flavoenzyme-Mediated Sulfur Dioxide Capture. *Angew. Chem., Int. Ed.* **2015**, *54*, 13279−13283.

(48) Dokainish, H. M.; Gauld, J. W. Formation of a Stable Iminol Intermediate in the Redox Regulation Mechanism of Protein Tyrosine Phosphatase 1B (PTP1B). *ACS Catal.* **2015**, *5*, 2195−2202.

(49) Wan, Y.; Fang, G.; Chen, H.; Deng, X.; Tang, Z. Sulfonamide derivatives as potential anti-cancer agents and their SARs elucidation. *Eur. J. Med. Chem.* **2021**, *226*, No. 113837.

(50) Huang, F.; Nau, W. M. A conformational flexibility scale for amino acids in peptides. *Angew. Chem., Int. Ed.* **2003**, *42*, 2269−2272.

◼ NOTE ADDED AFTER ASAP PUBLICATION

This paper originally published ASAP on May 11, 2023. An error in the TOC graphic was corrected and a new version reposted May 23, 2023.